Modelling toluene oxidation

Hoorn, J.A.A.; van Soolingen, J.; Versteeg, G. F.

Published in:
Chemical Engineering Research and Design

DOI:
10.1205/cherd.04161

Publication date:
2005

IChemE

www.icheme.org/journals
doi: 10.1205/cherd.04161

0263–8762/05/$30.00+0.00

Trans IChemE, Part A, February 2005
Chemical Engineering Research and Design, 83(A2): 187–195

MODELLING TOLUENE OXIDATION
Incorporation of Mass Transfer Phenomena

J. A. A. HOORN[1]*, J. VAN SOOLINGEN[1] and G. F. VERSTEEG[2]

[1]*DSM Research, Geleen, Netherlands*
[2]*Department of Chemical Engineering, University of Twente, Enschede, Netherlands*

The kinetics of the oxidation of toluene have been studied in close interaction with the gas–liquid mass transfer occurring in the reactor. Kinetic parameters for a simple model have been estimated on basis of experimental observations performed under industrial conditions. The conclusions for the mass transfer and reaction regime on basis of experimental observations and model calculations are in good agreement: toluene oxidation under industrial conditions can be characterized as a slow reaction with respect to mass transfer.

Keywords: chemical reactors; kinetics; mass transfer; mathematical modelling; multiphase reactions; reaction engineering.

INTRODUCTION

The site of DSM Special Products Rotterdam has the largest toluene oxidation plant in the world, producing benzoic acid that for the major part is converted to phenol. In addition, benzoic acid and its derivative sodium benzoate also find their applications in the food and fine chemicals industry. The DSM site at Rotterdam also has the largest production unit for benzaldehyde, a specialty chemical. Since the development of the process (Keading *et al.*, 1965) a large number of studies on the chemistry of toluene oxidation and related hydrocarbons have been published. Most of the earlier publications have in common that the main focus is on the kinetics and that other process items are not considered (Borgaonkar *et al.*, 1984; Lozar *et al.*, 2001; Mulkay and Rouchaud, 1967; Quiroga *et al.*, 1980; Scott and Chester, 1972). This approach is not sufficient when considering scale-up and modelling of the plant reactors. For safety reasons, oxygen levels in the reactor off-gas have to be kept below the explosion limits. This means that at least in part of the reactor the oxygen partial pressure is so low that the liquid concentration is significantly decreased. In the range of low oxygen concentrations, the radical chain mechanism produces different by-products (Bateman, 1951). In addition, it is expected that the mass transfer of oxygen influences the productivity of the reactor. It is essential to quantify kinetics in close interaction with the mass transfer phenomena occurring in the reactor in order to increase the control of the productivity and selectivity.

**Correspondence to*: J. A. A. Hoorn, DSM Research, CT&A-ACES, PO Box 18, 6160 MD Geleen, The Netherlands.
E-mail: johan.hoorn@dsm.com

KINETICS AND MASS TRANSFER

The oxidation of toluene with air at elevated temperatures and pressures proceeds via a mechanism consisting of a chain of radical reactions and is initialized by cobalt ions. The use of elementary reactions in this radical mechanism is at this moment too complicated (lack of basic data and the need for extensive numerical solving techniques) to be of much practical use in the analyses on mass transfer and reaction. Instead a more simplified kinetic description is applied in the present study. The kinetic scheme in Figure 1 is directly derived from the stoichiometric equations (assuming elementary reactions) and has been proposed earlier for toluene oxidation (Quiroga *et al.*, 1980) as well as xylene oxidation (Cao *et al.*, 1994). For oxidation reactions proceeding through radical intermediates, a zero-order reaction rate is commonly encountered (Helfferich, 2001). Morimoto and Ogata (1967) concluded from their batch experiments that for oxygen levels below 42 vol% (the oxygen concentration in the reactor was kept constant by maintaining a constant pressure through suppletion of pure oxygen to the oxygen/nitrogen mixture) the reaction order in oxygen can be taken as one, whereas at higher oxygen levels the order is zero. Bhattacharya *et al.* (1973) give a reaction order for oxygen of $\frac{1}{2}$, but the experimental conditions are not fully given. The rates for the reactions in Figure 1 are assumed to be first-order in the reactants, also for oxygen. As it mathematically can be shown, it is not possible to determine the individual rate constants for reactions 1, 2 and 4 independently without experiments comprising benzyl alcohol added to the feed. These experiments have not been performed while the availability of the experimental set-up for kinetic experiments was very limited. In addition, benzyl alcohol is

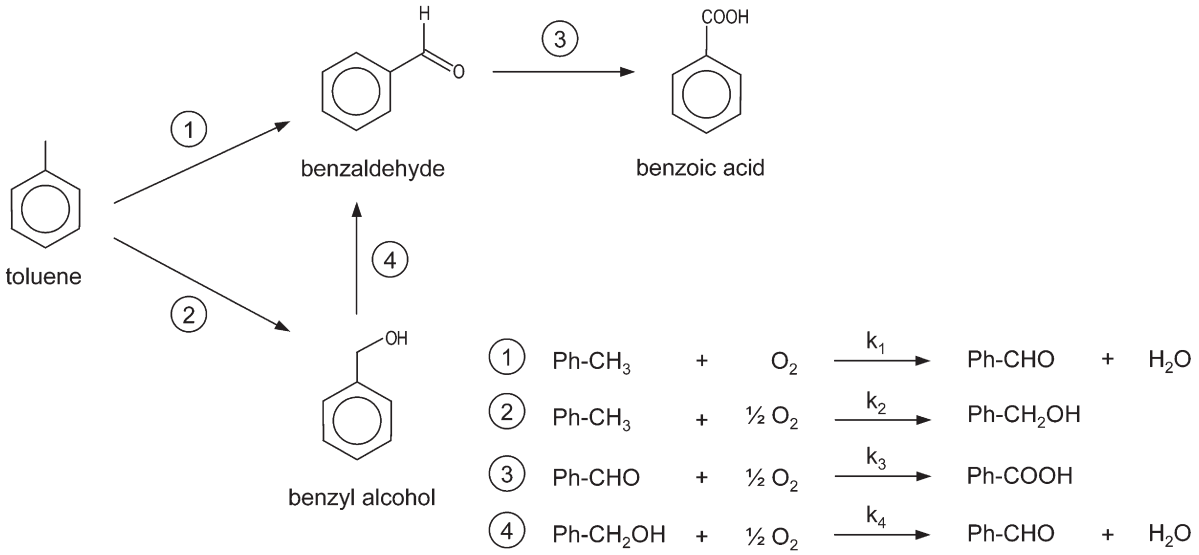

Figure 1. Basic scheme for the kinetics.

known to inhibit the oxidation (Morimoto and Ogata, 1967) making the operation of a continuous tank reactor more difficult than it is already. A correlation between R_1 and R_2 was made on basis of the observation that in the oxidation mechanism the primary termination reaction takes place between two alkoxy radicals (Russell, 1957; Kondratiev, 1969) whereby alcohol and aldehyde are formed in a 1 : 1 ratio. For this reason, the parameters k_1 and k_2 were replaced by a single parameter k_{12} giving the following expressions for the reaction rates:

$$R_1 = k_{12} \cdot c_{\mathrm{TOL}} \cdot c_{\mathrm{O2}} \tag{1}$$

$$R_2 = k_{12} \cdot c_{\mathrm{TOL}} \cdot c_{\mathrm{O2}} \tag{2}$$

$$R_3 = k_3 \cdot c_{\mathrm{BALD}} \cdot c_{\mathrm{O2}} \tag{3}$$

$$R_4 = k_4 \cdot c_{\mathrm{BALC}} \cdot c_{\mathrm{O2}} \tag{4}$$

The influence of the catalyst was not included in the rate equations because all experimental data have been performed at a constant cobalt concentration. The expression for the Hatta number (φ) depends on the reaction rate equation. For a first-order irreversible reaction with respect to the absorbing component φ is defined by:

$$\varphi = \frac{\sqrt{k \cdot D}}{k_{\mathrm{L}}} \tag{5}$$

For systems consisting of multiple reactions involving the gaseous component the most commonly applied simplification is to evaluate the Hatta number on the assumption that an overall pseudo zero-order or first-order rate equation is applicable. The model of the xylene oxidation by Cao *et al.* (1994) comprises a zero order reaction for oxygen where Hatta is calculated according to the correlation of Hikita and Asai (1964). This approach is also applied by Suresh *et al.* (1988) in the modelling of the cyclohexane oxidation. Pohorecki *et al.* (2001) apply a first order dependence for oxygen in the cyclohexane oxidation with a kinetic scheme that has a close resemblance to the toluene oxidation scheme given in Figure 1. The mass transfer flux for a first-order irreversible reaction according to the Danckwerts modification of the penetration theory is defined by (Westerterp *et al.*, 1984):

$$J = k_{\mathrm{L}} \cdot \left[c_{\mathrm{A,i}} - \frac{c_{\mathrm{A,b}}}{1 + \varphi^2} \right] \cdot \sqrt{1 + \varphi^2} \tag{6}$$

The extremes for small and large Hatta numbers are convenient for simple evaluations on basis of analytical solutions.

$$\varphi > 2 \quad J = k_{\mathrm{L}} \cdot c_{\mathrm{A,i}} \cdot \varphi \tag{7}$$

$$\varphi < 0.3 \quad J = k_{\mathrm{L}} \cdot (c_{\mathrm{A,i}} - c_{\mathrm{A,b}}) \tag{8}$$

The enhancement factor is the ratio of the flux in presence of reaction [equation (6)] and pure physical mass transfer under identical conditions [expression is equivalent to equation (8)].

$$E = \sqrt{1 + \varphi^2} \cdot \frac{\left(c_{\mathrm{A,i}} - (c_{\mathrm{A,b}})/(1 + \varphi^2)\right)}{c_{\mathrm{A,i}} - c_{\mathrm{A,b}}} \tag{9}$$

The extremes for small and large Hatta numbers are:

$$\varphi > 2 \quad E = \varphi \tag{10}$$

$$\varphi < 0.3 \quad E = 1 \tag{11}$$

The Hatta number and the enhancement factor are calculated from experimental observations, respectively included in the modelling.

EXPERIMENTS AND OBSERVATIONS

The reactor and auxiliary equipment for the toluene oxidation experiments are operated in a continuous mode,

a schematic drawing of the set-up is given in Figure 2. All equipment is accommodated in an explosion proof facility. From the continuous monitoring of the reactor temperature and the oxygen concentration in the off-gas during experiments it appeared that small fluctuations are present in the reaction set-up. The standard deviations of the results of five reference experiments having identical process conditions are shown in Table 1 as an indication of the extent of experimental inaccuracies. The range of process variables of all experiments is included for comparison. A number of experiments have been performed with insufficient tracing in part of the piping from the reactor vessel to the condenser causing a partial condensation of the vapour and subsequent reflux of components to the reactor. The rate of oxygen transferred to the liquid phase (F_{GL}) was calculated from the difference between the gas feed and off-gas flow. Both the liquid and the gas phase were assumed to be ideally mixed; the residence times for the liquid were in the order of one hour. To address the gas phase mixing qualitatively a visual check was performed in an glass vessel comprising identical baffle and stirrer configuration. With cyclohexane as liquid at room temperature and nitrogen as gas feed, it was observed that at 1600 rpm stirrer speed a significant amount of gas backmixing occured into the liquid by means of vortex formation around the stirrer and turbulences behind the baffles. In addition, it was assumed that no oxygen is present in the liquid feed and the system operates at steady state. The oxygen concentration in the liquid at saturation was calculated according to Henry's law. The Henry coefficients were calculated from gas–liquid equilibirum data retrieved from the Dortmund Data Bank (program version DDBSP 2003; http://www.ddbst.com, president and CEO of DDBST is Prof. Dr J. Gmehling, access date 26 November 2004). Typical values are in the range of 1500–2000 bar. The partial pressure of oxygen was determined from the off-gas and condensate composition. In Figure 3 the conversion rates for oxygen are shown as function of the oxygen concentration in the liquid. The conversion rate for oxygen is defined as the transfer rate of oxygen divided by the liquid volume; in this way the outflow of dissolved oxygen is neglected. The experimentally observed oxygen transfer rate F_{GL} is related with the flux through the interfacial area:

$$F_{GL} = J \cdot V_R \cdot a \tag{12}$$

In case $\varphi > 2$ substitution of the expression for the observed transfer rate gives (taking into account the definition for the Hatta number):

$$k = \frac{1}{D} \cdot \left(\frac{F_{GL}}{V_R \cdot a \cdot c_{A,i}} \right)^2 \tag{13}$$

For $\varphi < 0.3$ the bulk concentration can be calculated from a balance for oxygen in the liquid phase:

$$0 = -\phi_V \cdot c_{A,b} - (1-\varepsilon) \cdot V_R \cdot k \cdot c_{A,b} + J \cdot V_R \cdot a \tag{14}$$

The outflow of dissolved oxygen is considered to be much smaller than the reaction term and the transfer rate through the gas–liquid interface; therefore equation (14) can be simplified to:

$$0 = -(1-\varepsilon) \cdot V_R \cdot k \cdot c_{A,b} + J \cdot V_R \cdot a \tag{15}$$

with the substitution for J [equation (8)]:

$$\frac{c_{A,b}}{c_{A,i}} = \frac{1}{1 + Al \cdot \varphi^2} \tag{16}$$

where Al is the Hinterland ratio:

$$Al = \frac{(1-\varepsilon) \cdot k_L}{a \cdot D} \tag{17}$$

Combining the expression for the bulk concentration with the flux and the observed conversion rate gives an equation that can be solved with respect to the kinetic rate constant:

$$F_{GL} = V_R \cdot a \cdot k_L \cdot \left(c_{A,i} - \frac{c_{A,i}}{1 + Al \cdot \varphi^2} \right) \tag{18}$$

Solving for k gives:

$$k = \frac{k_L^2}{Al \cdot D} \cdot \frac{F_{GL}}{V_R \cdot k_L \cdot a \cdot c_{A,i} - F_{GL}} \tag{19}$$

Values for specific surface areas were estimated with the correlation of Shridhar and Potter (1980), diffusion coefficients were estimated with the correlation of Wilke and Chang (1955). Mass transfer coefficients were estimated for water with the equation of van't Riet (1979). To translate the mass transfer coefficients from water to toluene at reactor conditions, a result from Higbie's penetration theory was applied:

$$\frac{k_L(\text{toluene}, 150^\circ\text{C})}{k_L(\text{water}, 25^\circ\text{C})} = \sqrt{\frac{D(\text{toluene}, 150^\circ\text{C})}{D(\text{water}, 25^\circ\text{C})}} \tag{20}$$

The experimental conditions in the experiments were such that the volumetric mass transfer coefficient could be taken as constant at a value of 0.75 s^{-1}. The interfacial

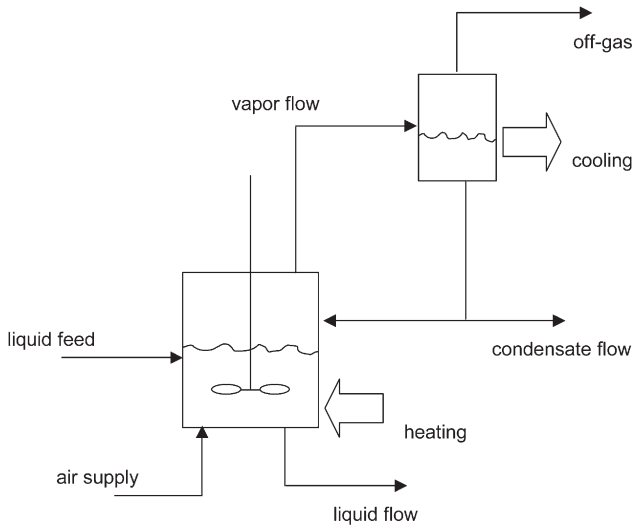

Figure 2. Experimental set-up.

Table 1. Data from a series of standard experiments.

			Range of operation including all experiments	Standard deviation in reference experiments
Reactor temperature		°C	140–160	0.8%
Reactor pressure		bar	4–7	0.2%
Off-gas inert flow		Nl/h	100–300	1.1%
Feed flow toluene		kg/h	1–2	1.0%
Feed flow air		Nl/h	100–300	0.3%
Flow liquid discharge		kg/h	0.5–1.5	2.1%
Flow condensate		kg/h	0.5–1.5	2.3%
Off-gas oxygen level		vol%	0–6	32.5%
Condensate	Balc	mol/h	0.0003–0.005	12.5%
	Bald	mol/h	0.003–0.02	7.3%
	BzA	mol/h	0–0.02	20.8%
	H_2O	mol/h	0.6–1.6	11.0%
	Tol	mol/h	2.1–5.6	4.8%
Liquid discharge	Balc	mol/h	0.003–0.05	3.9%
	Bald	mol/h	0.03–0.2	1.8%
	BzA	mol/h	0.4–1.1	3.3%
	Tol	mol/h	1.5–10.9	1.5%

area was taken as a constant at $300\,m^2/m^3$. Under the hypothesis that the reaction is fast, i.e., $\varphi > 2$, the calculated rate constant [equation (13)] is $100\,s^{-1}$ ($\pm 56\,s^{-1}$, standard deviation for the experimental observations). The corresponding Hatta number on basis of this rate constant can then be estimated to be 0.60 ± 0.16. This is not in line with the assumption of a fast reaction with $\varphi > 2$. For the hypothesis of a slow reaction, i.e., $\varphi < 0.3$, the calculated rate constant is $2.2 \pm 3.2\,s^{-1}$ giving a Hatta number of 0.079 ± 0.048 which is in line with the assumption made for the Hatta number. Therefore, it is concluded that on basis of the experimental observations the reaction rate is slow in comparison to the mass transfer rate of oxygen.

MODELLING OF THE EXPERIMENTAL REACTOR

A model was constructed to determine the kinetic parameters under conditions of mass transfer limitations while taking into account partial condensation of the vapour phase. To include a description of the partial condensation between the reactor and the condenser the model comprised two flash calculations for the reactor part of the set-up. A scheme of the model is given in Figure 4. For an overview on the model equations see Appendix. The model calculations were performed in Aspen Custom Modeler. Thermodynamic properties for the liquid phase were calculated with Aspen Plus Properties. The pure component properties were taken from the DIPPR Handbook (http://dippr.byu.edu, American Institute of Chemical Engineers, access date 25 May 2004) or DDBST (http://www.ddbst.com). The interaction between components was described by the NRTL-model. The thermodynamic property files generated in Aspen Plus were included in the ACM file. The liquid from the second flash is totally refluxed to the first flash ('liquid recycle'). The temperature of the second flash was varied for each experiment in such a way that the differences between experimental and model values for the gas and liquid mole flows of all components were minimized. The calculations to determine the temperatures of the second flash were performed with a simulated combined feed of the liquid discharge and vapour flows. For experiments performed with the correct tracing, the temperature of the second flash was fixed at the temperature of the first

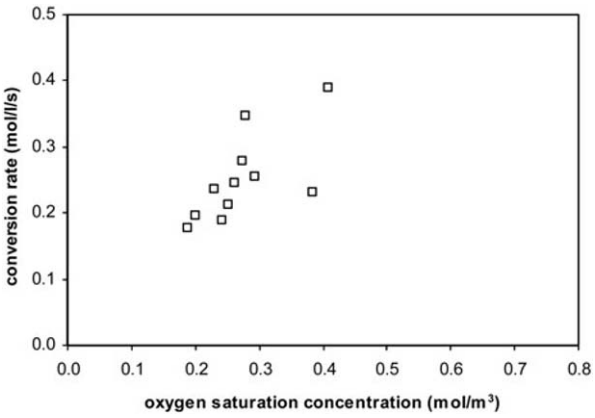

Figure 3. Observed conversion rates for oxygen as function of the oxygen concentration in the liquid at saturation.

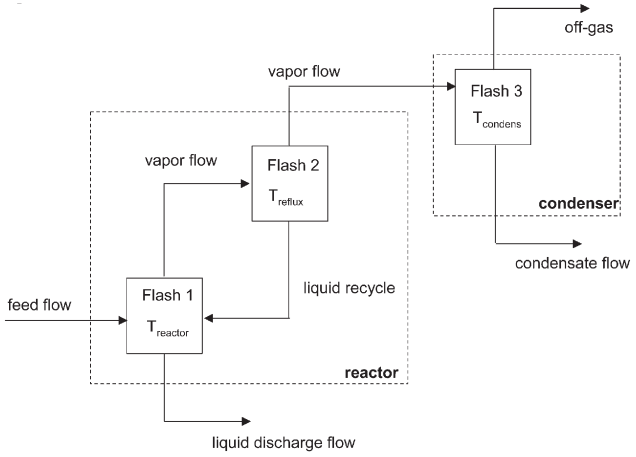

Figure 4. Schematic drawing of model. The symbols in this scheme are utilized in the overview of model equations.

Table 2. Statistics for vapour–liquid calculations.

		SSO (mol^2/h^2)	SSR (mol^2/h^2)	Standard deviation	SSR without reflux (mol^2/h^2)	Standard deviation without reflux
Condensate	Balc	$3.24 \cdot 10^{-5}$	$5.61 \cdot 10^{-6}$	35.5%	$8.74 \cdot 10^{-5}$	127.5%
	Bald	$9.29 \cdot 10^{-4}$	$1.69 \cdot 10^{-4}$	21.7%	$1.38 \cdot 10^{-3}$	61.3%
	BzA	$4.45 \cdot 10^{-4}$	$1.87 \cdot 10^{-4}$	34.2%	$1.34 \cdot 10^{-4}$	37.3%
	H_2O	$1.26 \cdot 10^{1}$	$2.23 \cdot 10^{-1}$	11.0%	$2.57 \cdot 10^{-1}$	12.6%
	Tol	$1.61 \cdot 10^{2}$	$2.72 \cdot 10^{0}$	11.0%	$3.34 \cdot 10^{1}$	36.1%
Liquid discharge	Balc	$6.92 \cdot 10^{-3}$	$5.61 \cdot 10^{-6}$	2.4%	$8.74 \cdot 10^{-5}$	9.4%
	Bald	$1.53 \cdot 10^{-1}$	$1.69 \cdot 10^{-4}$	3.0%	$1.38 \cdot 10^{-3}$	8.7%
	BzA	$5.09 \cdot 10^{0}$	$1.87 \cdot 10^{-4}$	0.5%	$1.34 \cdot 10^{-4}$	0.4%
	Tol	$4.84 \cdot 10^{2}$	$2.72 \cdot 10^{0}$	11.0%	$3.34 \cdot 10^{1}$	38.5%

flash. The temperatures of the second flash were 5 to 15°C lower than the reactor temperature depending on the composition of the condensate flow. The liquid recycle amounts to 10–20% (mole flow basis) compared to the vapour flow feeding the second flash. The statistical results of the calculations are given in Table 2. The kinetic parameters in Figure 1 were estimated by a least squares minimization procedure. In the estimation procedure (and in the subsequent model calculations) the temperatures in the second flash were fixed at the values calculated earlier. The most suitable variables as experimental data points and the optimal weighting were identified after some trial and error. Best results were obtained with the toluene conversion, selectivities for benzyl alcohol, benzaldehyde and benzoic acid and the oxygen off-gas concentration. The weights of the experimental values for a particular variable were set as reciprocals of the average values, except for oxygen which was given a lower value (10% of the reciprocal average). The results are given in Table 3. In Table 4 the sums of the squared residuals of model prediction and experimental values (SSR) are shown. The model results for the data applied in the estimation procedure are shown in the parity plots in Figures 5–8. Comparison between experimental values and model calculations for the oxygen concentration in the off-gas are shown in Figure 9. The residuals for benzyl alcohol, benzaldehyde and benzoic acid selectivity are shown in Figures 10 and 11. Residual values are given as the difference in selectivity between experiment and model relative to the observed experimental value. The calculated pseudo first-order rate constant is $k_{fo} = 295 \pm 14\ s^{-1}$, the Hatta number is $\varphi = 0.92 \pm 0.05$ and the enhancement factor is $E = 1.36 \pm 0.03$.

Table 3. Estimated parameter values and correlation matrix.

Parameter values			Reactions	Correlation matrix			
k_{12}	0.015 ± 0.004	$m^3/mol/s$	Tol → Balc		k_{12}	k_3	k_4
			Tol → Bald	k_{12}	1		
k_3	1.35 ± 0.36	$m^3/mol/s$	Bald → BzA	k_3	0.98	1	
k_4	3.9 ± 1.0	$m^3/mol/s$	Balc → Bald	k_4	0.99	0.98	1

Table 4. Sum of squares for experiments and model.

	Experiment SSO	Model SSR
O_2 off-gas	$7.2 \cdot 10^{1}$	$4.3 \cdot 10^{1}$
Tol conversion	$7.2 \cdot 10^{-2}$	$1.8 \cdot 10^{-3}$
Balc selectivity	$9.6 \cdot 10^{-3}$	$1.4 \cdot 10^{-4}$
Bald selectivity	$2.4 \cdot 10^{-1}$	$1.7 \cdot 10^{-3}$
BzA selectivity	$7.5 \cdot 10^{0}$	$1.6 \cdot 10^{-3}$

DISCUSSION

From Table 1 it appears that the input process parameters are controlled with acceptable accuracy of approximately 1%. The response variables differ in accuracy in the range of 1.5% for toluene in the liquid discharge flow to 20% for benzoic acid in the condensate flow. Benzoic acid concentrations in the condensate flow are difficult to analyse because at room temperature the condensate separates into a water and an organic phase. The low accuracy for the oxygen measurement is a combination of the analytical measurement and the length of the sample pipe from the off-gas vessel to the instrument. The simulation of the partial condensation in the piping to the condenser vessel is successfully performed by modelling the reactor part with an additional flash calculation (Figure 4) and this is illustrated when the results in Table 2 are compared. The differences between model predictions and experimental observations are clearly reduced with respect to the situation where there is no liquid recycle. When compared to the indication of experimental errors in Table 1, the model describing the partial condensation has a scatter in the model predictions that is much closer to the

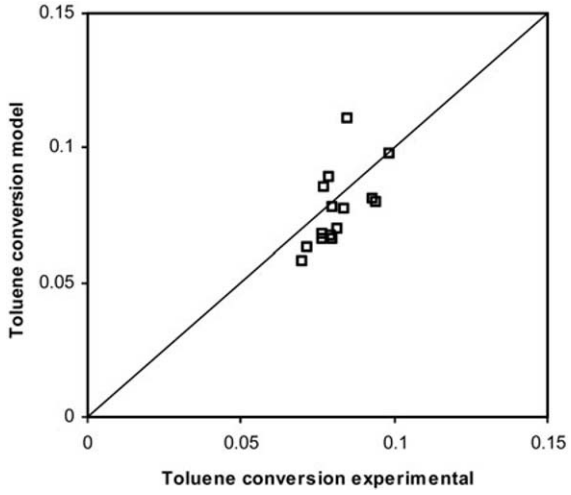

Figure 5. Comparison between experimental values and model calculations for the conversion of toluene.

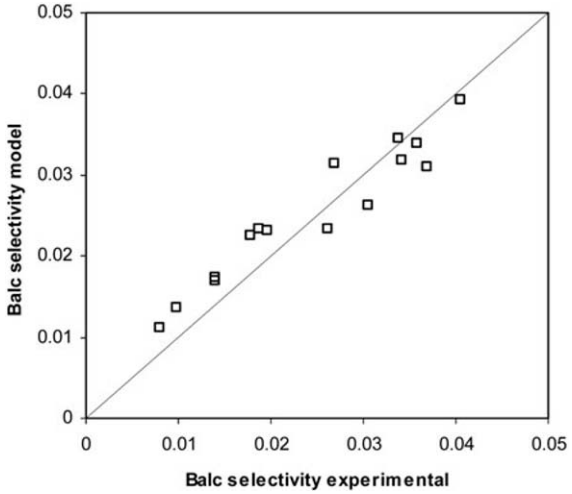

Figure 6. Comparison between experimental values and model calculations for the selectivity of benzyl alcohol.

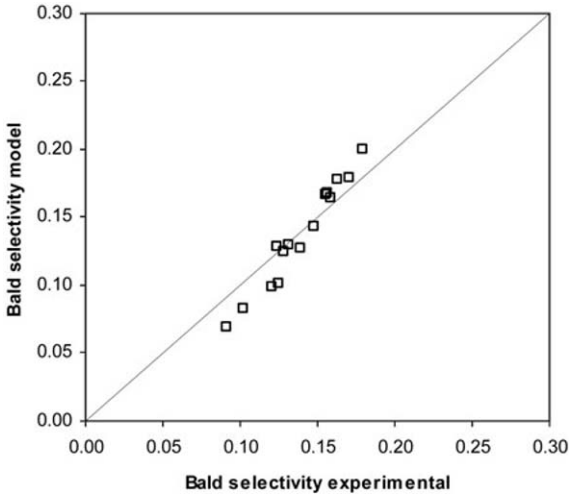

Figure 7. Comparison between experimental values and model calculations for the selectivity of benzaldehyde.

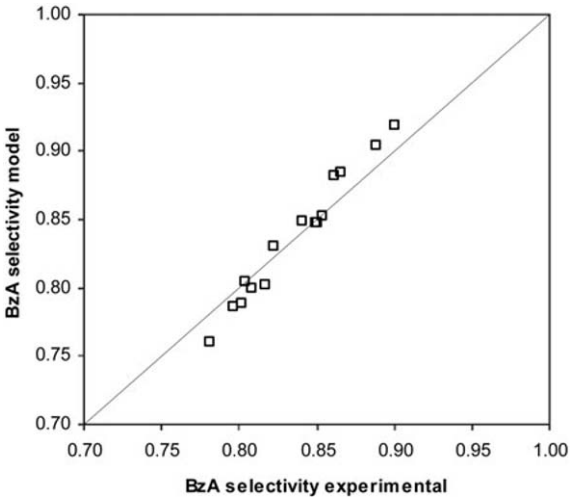

Figure 8. Comparison between experimental values and model calculations for the selectivity of benzoic acid.

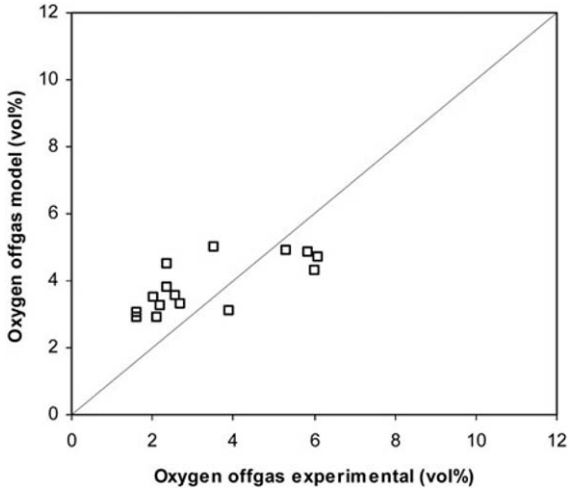

Figure 9. Comparison between experimental values and model calculations for the oxygen concentration in the off-gas.

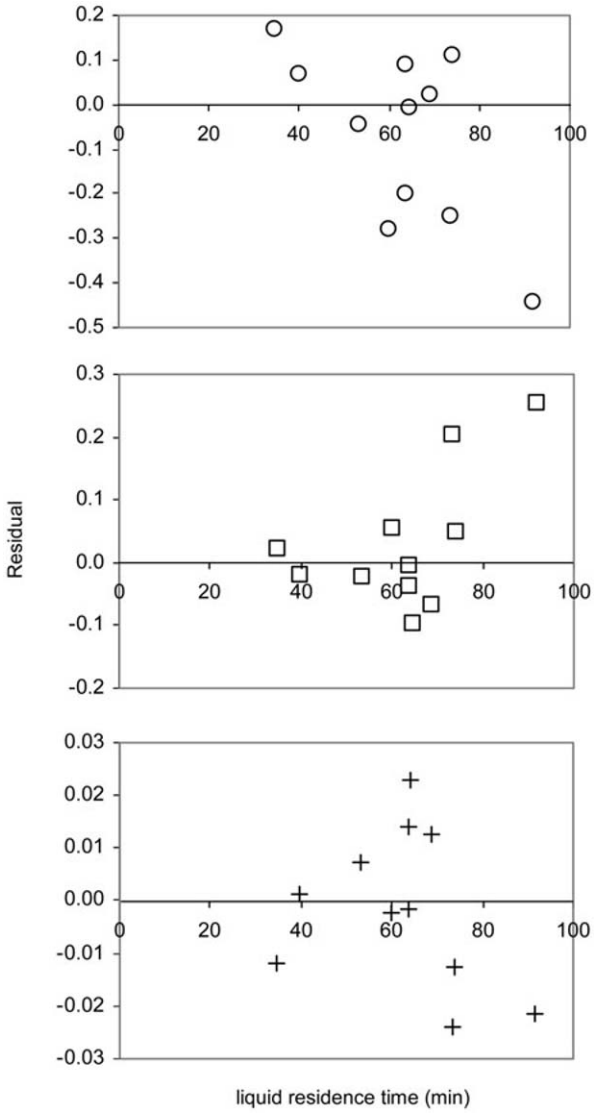

Figure 10. Residuals between experimental and model values as function of the residence time based on the liquid feed flow rate; (○) = benzyl alcohol; (□) = benzaldehyde; (+) = benzoic acid.

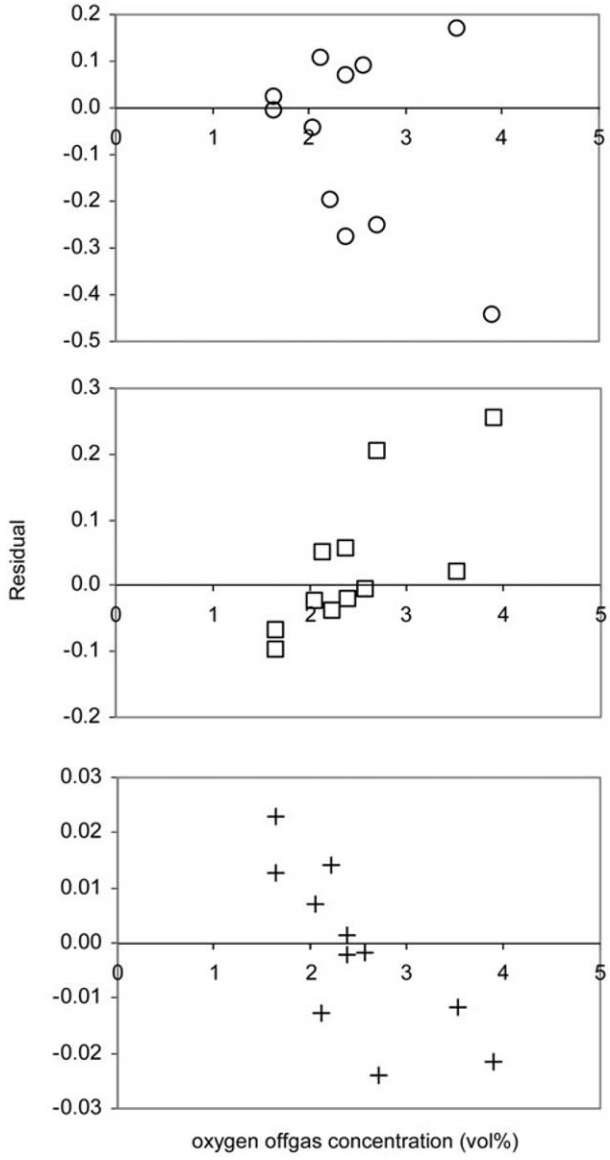

Figure 11. Residuals between experimental and model values as function of the experimental observed oxygen concentration in the off-gas; (○) = benzyl alcohol; (□) = benzaldehyde; (+) = benzoic acid.

experimental error than the model version without the reflux mechanism. Tables 3 and 4 summarize results of the estimated kinetic parameters. The values of the standard deviations as well as the correlation parameters are in acceptable limits for further scale-up purposes, but improvement is still desired. The residual sums are acceptable in comparison to the experimental values. This picture is confirmed by the graphs of the residual plots of the toluene conversion and the selectivity's of benzyl alcohol, benzaldehyde and benzoic acid (Figures 5–8). The parity plot for oxygen exhibits a fair off-set (Figure 9). This is caused by the low weighting value for oxygen which was based on the inaccuracy of the experimental value. The residuals are larger when the liquid residence time increases or when the oxygen concentration is higher. (There is no direct relation between liquid residence time and oxygen concentration because the gas flow rate is set independent of the liquid feed flow rate.) For the determination of the reaction rate order in oxygen the results in Figure 3 do not exclude other than simple first order kinetics. The choice for a first-order oxygen dependence is quite arbitrary and has been done for practical reasons, a zero-order model is more difficult to handle because of the discontinuities with the reaction rates. When some reaction rate equation other than a power law is required to improve the model accuracy, mass transfer rates have to be solved by numerical procedures. The combination of these numerical solutions with parameter estimation procedures has not been performed so far. The value of the Hatta number that was directly derived from the experimental observations indicates that the oxidation of toluene can be considered to be slow. The Hatta number of 0.09 derived from the experimental observations is in good agreement with the value calculated with the model. The enhancement factor calculated by the model is also close to unity. The results obtained with the model show a more narrow distribution of errors. The standard deviations in the average Hatta number is smaller (5% relative) than with the experimentally determined Hatta number (50%). The low values of Hatta and the enhancement factor imply the presence of an oxygen concentration in the liquid bulk, suggesting that reaction of oxygen with some kind of radical intermediate can not be the rate-determining step in the overall mechanism. This is in general agreement with the picture for autoxidation reactions (Helfferich, 2001).

CONCLUSIONS

Experiments performed in a reactor that was operated under industrial conditions have been successfully applied in the estimation of kinetic parameters in a model with inclusion of the description of mass transfer phenomena. Analyses of the mass transfer characteristics reveal that toluene oxidation under industrial conditions is a slow reaction with respect to mass transfer.

NOMENCLATURE

a	interfacial area per unit volume of dispersion, m^2/m^3
Al	Hinterland ratio
c	concentration, $kmol/m^3$
$c_{A,b}$	concentration of A in the liquid bulk, $kmol/m^3$
$c_{A,i}$	concentration of A at the gas–liquid interface, $kmol/m^3$
$c_{O2,sat}$	saturation concentration of oxygen, $kmol/m^3$
$c_{O2,out}$	oxygen concentration in the gas outflow, $kmol/m^3$
D	diffusion coefficient, m^2/s
E	enhancement factor
F	flow, kmol/s
F_{GL}	flow across gas–liquid interface, kmol/s
J	flow across gas–liquid interface, $kmol/m^2/s$
k	reaction rate constant (second order), $m^3/kmol/s$
k	reaction rate constant (first order), s^{-1}
k_{fo}	reaction rate constant (pseudo first order), s^{-1}
k_L	liquid side mass transfer coefficient, m/s
k_La	volumetric liquid side mass transfer coefficient, 1/s
n	reaction order
p	partial pressure, bar
P_{tot}	total pressure (absolute), bar
R	reaction rate, $kmol/m^3/s$
V_R	dispersion volume (liquid + gas), m^3
w	mole fraction in liquid, mol/mol
x	mole fraction in liquid, mol/mol

$x_{O2,sat}$	oxygen mole fraction in liquid at saturation, mol/mol
y	mole fraction in vapour, mol/mol
z	mole fraction in vapour, mol/mol

Greek symbols

ε	gas volume per unit volume dispersion, m^3/m^3
χ	conversion, mol/mol
ϕ	fugacity coefficient
ϕ_V	volumetric flow, m^3/s
φ	Hatta number
$\rho_{mol,L}$	liquid molar density, $kmol/m^3$
σ	selectivity, mol/mol
τ_L	residence time, s

Sub/superscripts (see also Figure 4 for descriptions)

i	any component
BALC	benzyl alcohol
BALD	benzaldehyde
BzA	benzoic acid
H2O	water
N2	nitrogen
O2	oxygen
TOL	toluene
F	feed flow to Flash 1
G	gas vapour flow from Flash 2
L	liquid discharge flow from Flash 1
V	vapour flow from Flash 1 to Flash 2
R	liquid recycle flow from Flash 2 to Flash 1

Abbreviations

ACM	Aspen Custom Modeler
SSO	Sum of Squared Observations
SSR	Sum of Squared Residuals

REFERENCES

Bateman, L., 1951, Olefin oxidation. *Quart Revs (London)*, 8: 147–167.

Bhattacharya, D., Guha, D.K., Roy, A.N., 1973, Liquid phase air oxidation of toluene to benzoic acid. II. Kinetics and mechanism. *Chem Age India*, 24: 87–90.

Borgaonkar, H.V., Raverkar, S.R., Chandalia, S.B., 1984, Liquid phase oxidation of toluene to benzaldehyde by air. *Ind Eng Chem Prod Res Dev*, 23: 455–458.

Cao, G., Servida, A., Pisu, M., Morbidelli, M., 1994, Kinetics of p-xylene liquid-phase catalytic oxidation. *AIChE J*, 40: 1156–1166.

Helfferich, F.G., 2001, Kinetics of homogeneous multistep reactions, in Compton, R.G. and Hancock, G. (eds). *Comprehensive Chemical Kinetics, vol. 38*, 283–286 (Elsevier, Amsterdam, The Netherlands).

Hikita, H., Asai, S., 1964, Gas absorption with (m,n)-th order irreversible chemical reaction. *Int Chem Eng*, 4: 332–340.

Keading, W.W., Lindblom, R.O., Temple, R.G., Mahon, H.I., 1965, Oxidation of toluene and other alkylated aromatic hydrocarbons to benzoic acids and phenols. *Ind Eng Chem Process Des Dev*, 4: 97–101.

Kondratiev, V.N, 1969, The theory of kinetics, in Bamford, C.H. and Tipper, C.F.H. (eds). *Comprehensive Chemical Kinetics, vol. 2*, 165–173 (Elsevier, Amsterdam, The Netherlands).

Lozar, J., Falgayrac, G., Savall, A., 2001, Kinetics of the electrochemically assisted autoxidation of toluene in acetic acid. *Ind Eng Chem Res*, 40: 6055–6062.

Morimoto, T., Ogata, Y., 1967, Kinetics of the autoxidation of toluene catalyzed by cobaltic acetate. *J Chem Soc (B)*, 62–66.

Mulkay, P., Rouchaud, J., 1967, Solvatation des catalyseurs d'oxydation en phase liquide homogène. *Bull Soc Chim Fr*, 12: 4653–4657.

Pohorecki, R., Baldyga, J., Moniuk, W., Podgórska, W., Zdrójkowski, A., Wierzchowski, P.T., 2001, Kinetic model of cyclohexane oxidation. *Chem Eng Sci*, 56: 1285–1291.

Quiroga, O.D., Gottifredi, J.C., Capretto de Castillo, M.E., 1980, Liquid phase catalytic toluene oxidation, formulation of a kinetic model. *Lat Am J Chem Eng Appl Chem*, 10: 77–88.

Russell, G.A., 1957, Deuterium-isotope effects in the autoxidation of aralkyl hydrocarbons. Mechanism of the interaction of peroxy radicals. *J Am. Chem Soc*, 79: 3871–3877.

van't Riet, K., 1979, Review of measuring methods and results in nonviscous gas-liquid mass transfer in stirred vessels. *Ind Eng Chem Process Des Dev*, 18: 357–364.

Scott, E.J.Y., Chester, A.W., 1972, Kinetics of the cobalt-catalyzed autoxidation of toluene in acetic acid. *J Phys Chem*, 76: 1520–1524.

Shridhar, T., Potter, O.E., 1980, Interfacial areas in gas-liquid stirred vessels. *Chem Eng Sci*, 35: 683–695.

Suresh, A.K., Sridhar, T., Potter, O.E., 1988, Autocatalytic oxidation of cyclohexane—mass transfer and chemical reaction. *AIChE J*, 34: 81–93.

Westerterp, K.R., van Swaaij, W.P.M., Beenackers, A.A.C.M., 1984, *Chemical reactor design and operation*, 371–377. (John Wiley & Sons, New York, USA).

Wilke, C.R., Chang, P., 1955, Correlation of diffusion coefficients in dilute solutions. *AIChE J*, 1: 264–270.

The manuscript was received 2 June 2004 and accepted for publication after revision 13 December 2004.

APPENDIX

Overall pseudo first-order rate constant for oxygen

$$k_{fo} = \frac{3}{2} \cdot k_{12} \cdot c_{TOL} + \frac{1}{2} \cdot (k_3 \cdot c_{BALD} + k_4 \cdot c_{BALC})$$

Definition of Hatta number and mass transfer equations

$$\varphi = \frac{\sqrt{k_{fo} \cdot D}}{k_L}$$

$$F_{GL} = J \cdot V_R \cdot a$$

$$E = \sqrt{1+\varphi^2} \cdot \frac{\left(c_{O2,sat} - (c_{O2})/(1+\varphi^2)\right)}{c_{O2,sat} - c_{O2}}$$

$$J = k_L \cdot \left(c_{O2,sat} - c_{O2}\right) \cdot E$$

Reaction rate expressions (according to Figure 1)

$$R_1 = k_{12} \cdot c_{TOL} \cdot c_{O2}$$

$$R_2 = k_{12} \cdot c_{TOL} \cdot c_{O2}$$

$$R_3 = k_3 \cdot c_{BALD} \cdot c_{O2}$$

$$R_4 = k_4 \cdot c_{BALC} \cdot c_{O2}$$

$$R_{BALC} = R_2 - R_4$$

$$R_{BALD} = R_1 - R_3 + R_4$$

$$R_{BzA} = R_3$$

$$R_{H2O} = R_1 + R_4$$

$$R_{O2} = -R_1 - \frac{1}{2} \cdot (R_2 + R_3 + R_4)$$

$$R_{TOL} = -R_1 - R_2$$

Definition for toluene conversion

$$\chi = \frac{F_{F,TOL} - \left(F_{L,TOL} + F_{G,TOL}\right)}{F_{F,TOL}}$$

Definition for benzoic acid, benzaldehyde and benzyl alcohol selectivity

$$\sigma_i = \frac{F_{L,i} + F_{G,i}}{\sum_j F_{L,j} + \sum_j F_{G,j}}$$

Definition for off-gas oxygen concentration

$$c_{O2,out} = \frac{F_{G,O2}}{F_{G,N2} + F_{G,O2}}$$

Mole fractions and concentrations for all components

$$c_i = \rho_{mol,L} \cdot x_i$$
$$x_i = \frac{F_{L,i}}{\sum_i F_{L,i}}$$
$$y_i = \frac{F_{G,i}}{\sum_i F_{G,i}}$$
$$z_i = \frac{F_{VAP,i}}{\sum_i F_{VAP,i}}$$
$$w_i = \frac{F_{REC,i}}{\sum_i F_{REC,i}}$$

Mass balances for all components except oxygen for Flash 1 and Flash 2 (see Figure 4)

$$\phi_{L,i} \cdot x_i = \phi_{V,i} \cdot z_i$$
$$\phi_{G,i} \cdot y_i = \phi_{R,i} \cdot w_i$$
$$F_{F,i} + F_{R,i} + V \cdot R_i = F_{L,i} + F_{V,i}$$
$$F_{V,i} = F_{G,i} + F_{R,i}$$

Mass balances for oxygen

$$\phi_{L,O2} \cdot x_{O2,sat} = \phi_{V,O2} \cdot z_{O2}$$
$$\phi_{G,O2} \cdot y_{O2} = \phi_{R,O2} \cdot w_{O2}$$
$$F_{F,O2} = F_{GL,O2} + F_{V,O2}$$
$$F_{GL,O2} + F_{R,O2} + V_R \cdot R_{O2} = F_{L,O2}$$
$$F_{V,O2} = F_{G,O2} + F_{R,O2}$$